Focal macular ERGs elicited by 10° or 15° stimulus from OMD patients. The waveform of the focal macular ERGs is a depolarizing pattern with a small *a*-wave, if any, and a relatively large *b*-wave [15]. Adapted with permission from Miyake Y. 'Electrodiagnosis of retinal diseases', Tokyo: Springer-Verlag; 2006

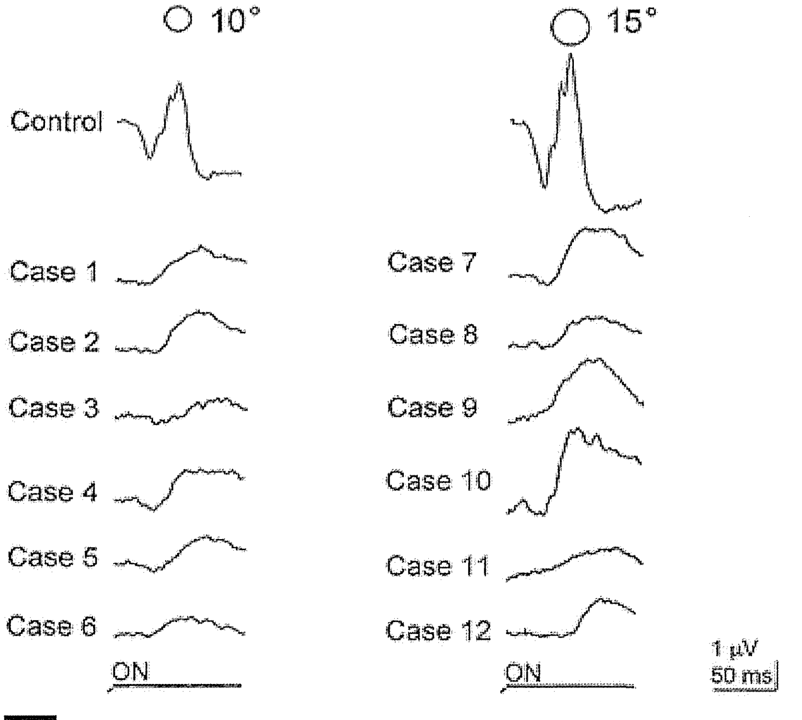

AQ1

A three-dimensional topographic map of the mfERGs is shown in Fig. 9. The averaged waveforms of the multifocal ERGs for the different eccentric rings in 20 normal subjects and 8 patients with OMD are superimposed [23]. The differences in the amplitudes of the ERGs recorded from patients with OMD and from normal subjects become smaller toward the peripheral field. Most OMD patients have slight but significantly longer implicit times than those of normal controls across the whole testing field. These longer implicit times suggest that the retinal dysfunction has a broader extent than expected from the ERG amplitudes and psychophysical perimetric results (see below).

Fig. 9

Three-dimensional topographic map (*left*) and averaged waveform (*right*) of multifocal ERGs for five eccentric rings in a normal subject and an

OMD patient [23]. Responses for 20 normal subjects and eight OMD patients are superimposed in the averaged waveforms. The *vertical dotted line* indicates an implicit time of 29.4 ms. Adapted with permission from Miyake Y. 'Electrodiagnosis of retinal diseases', Tokyo: Springer-Verlag; 2006

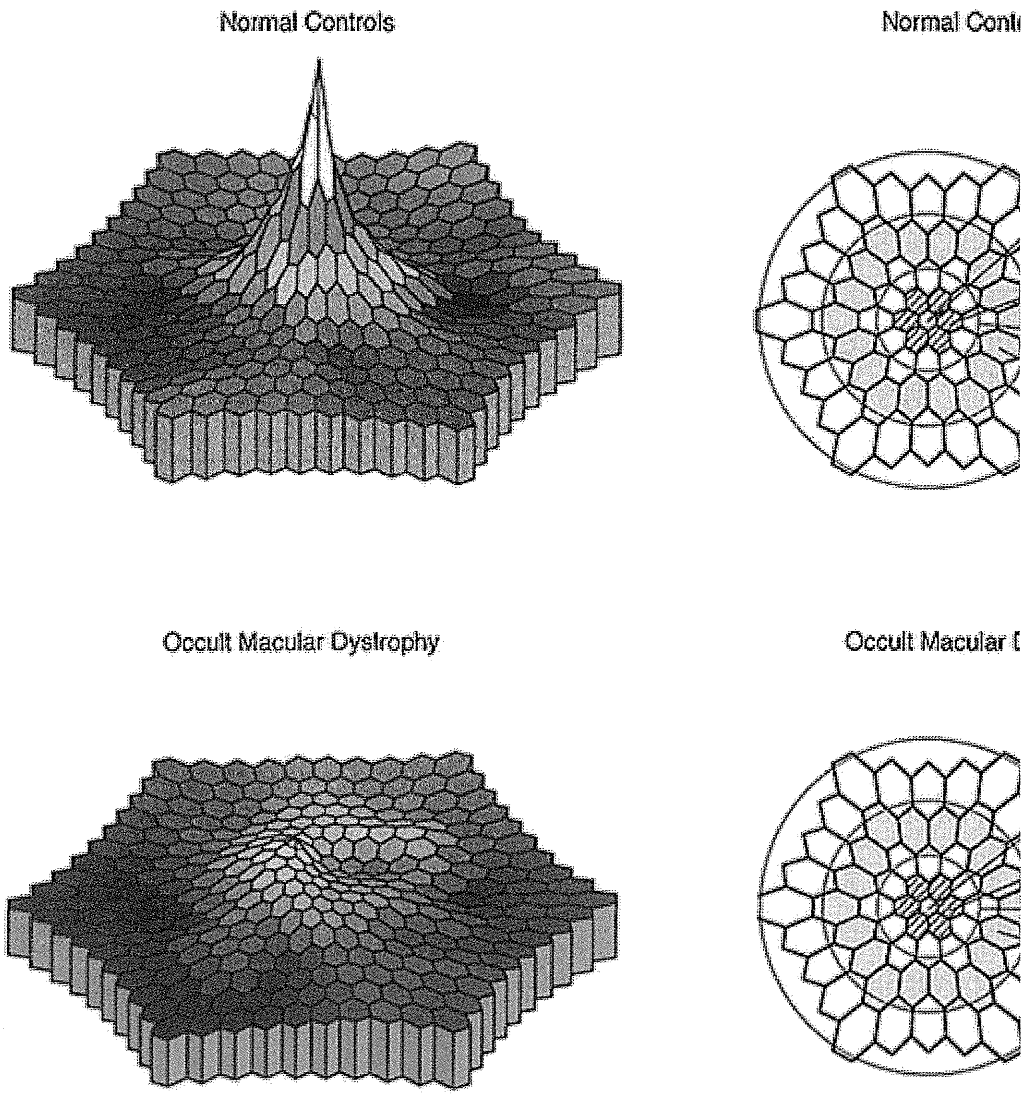

Two-color (cone-rod) perimetry in macula

Light-adapted (cone) and dark-adapted (rod) two-color perimetry is useful in the independent evaluation of the cone and rod visual pathways. This was originally designed by Jacobson and associates and is performed with a modified Humphrey Field Analyzer [35]. Only the function of the posterior pole was measured in our series [14]. Profile plots of cone-rod perimetry in a representative OMD patient (case 1) and cone perimetry in another OMD patient (case 2) are shown in Fig. 10. The visual acuity of case 1 was 0.2 and of case 2, 1.0. In each profile, the normal variations (mean ± 2 SD) of 30 normal subjects are shown as the range surrounded by the two dotted lines. The normal sensitivity level for the light-adapted test is at least 15 dB at all test points with higher levels near the center of the visual field. The light-adapted results indicate abnormal sensitivities only at the fovea. The normal dark-adapted sensitivity for the 500-nm target was approximately 70 dB with the lower level at the fovea, and approximately 40 dB for the 650-nm target. When the red (560-nm) and blue-green (500-nm) targets are adjusted for equal energy, the rod photoreceptor system will be 26 dB more sensitive to blue-green than to red, whereas cones will show only 8 dB greater sensitivity to blue–green than to red. Therefore, a sensitivity difference of approximately 26 dB indicates a rod-mediated detection, whereas a difference of approximately 6 dB means a cone-mediated detection. The sensitivity differences of between 8 and 26 dB suggest mixed rod and cone detection: rods detect the blue–green stimulus and cones the red stimulus. Based on these criteria, the macular cone sensitivity is depressed but rod sensitivity is normal in case 1. In case 2, the macular cone sensitivity is severely depressed, but a small area of the fovea has good sensitivity, resulting in normal visual acuity.

Fig. 10

Results of two-color perimetry. Rod-cone perimetry (*left*) and cone perimetry (*right*) in two patients with OMD. The visual acuity of cases 1 and 2 are 0.2 and 1.0, respectively. In case 1, the macular cone sensitivity is depressed severely, but macular rod sensitivity is within the normal range. In case 2, the macular cone sensitivity is depressed, but only a small area of the fovea has good sensitivity. The *dotted lines* (*left*) and *solid lines* (*right*) indicate the normal range. Adapted with permission from Miyake Y. ‘Electrodiagnosis of retinal diseases’, Tokyo: Springer-Verlag; 2006

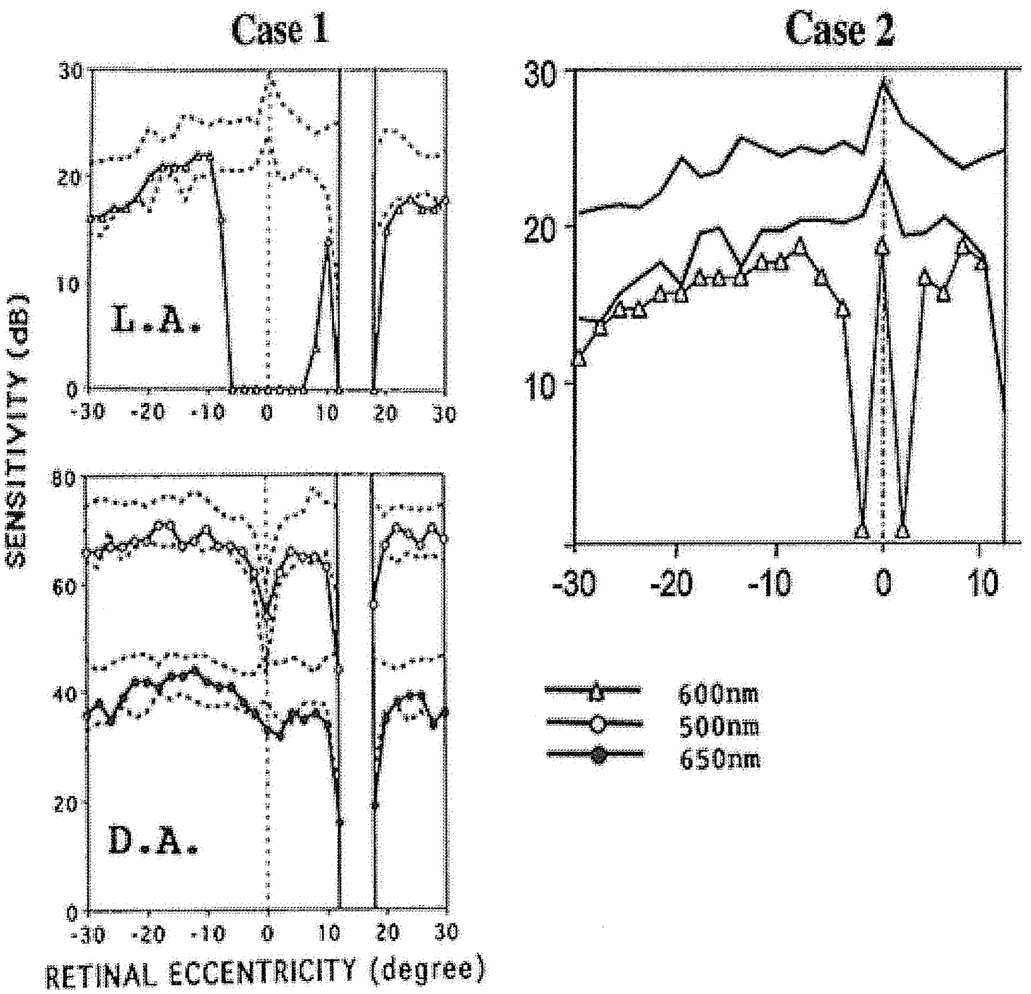

In our series of 13 patients with OMD who underwent this two-color perimetric testing, a loss in the sensitivity of the cone system in the macula was detected in all patients. The sensitivity of the macular rod system was normal in six patients (group 1), and borderline or abnormal in six patients (group 2). The average age of the patients was 30.2 years in group 1 and 58 years in group 2 ($P < 0.05$). These results suggest that only the cone system is abnormal in the relatively early stage, and the rod system is impaired in older patients.

Some patients have normal visual acuity in spite of having abnormal focal macular ERGs or multifocal ERGs (see case 2). This apparent discrepancy can be resolved by examining the cone sensitivity profile in Fig. 10. The patients with good visual acuity also had decreased cone sensitivity in the macula, but the function of one point in the foveola may still be relatively well preserved. It may be that the small center of the fovea in such patients functions well and accounts for the good visual acuity. The parafovea, however, is dysfunctional, resulting in the low amplitude in focal macular ERGs.

Optical coherence tomography

Spectral-domain OCT is a very important method in the diagnosis of OMD [30]. In patients with the *RP1L1* mutation, the most prominent features on OCT are the abnormalities of the two highly reflective lines in the OCT images at the macula.

These lines correspond to the ellipsoid region of the photoreceptor inner segments (ISe) and cone outer segment tips (COST) line (Fig. 11). The ISe line at the fovea appears thickened and blurred in the early stages of OMD and disrupted or absent in the later stages. The COST line cannot be clearly observed in the macular area even in the early stage. In the peri-macular regions which have normal visual function, all the outer retinal microstructures are normal. In longer duration cases, e.g., >30 years, both the photoreceptor and outer nuclear layers are thinnest at the macula; however, the retinal pigment epithelium remains unchanged (Fig. 11). The location of the COST line coincides with the location where the outer segment cone discs are renewed [36, 37], and the ISe line coincides with the region which is rich in mitochondria that play important roles in cellular metabolism [38]. The disappearance or blurring of both COST and ISe lines thus indicates an early stage of dysfunction of the cone photoreceptors.

Fig. 11

OCT images from two OMD patients with *RP1L1* mutation (p.Arg45Trp, heterozygous). **a** OCT image of a normal control without the *RP1L1* mutation (40-year-old man). All of the outer retinal structures, including ellipsoid of photoreceptor inner segment (ISe) line, cone outer segment tip (COST) line, and retinal pigment epithelium (RPE), are clearly observed both in the fovea and the peri-macular region. **b** A 30-year-old man. The COST line is not present over the entire macula but is present in the peri-macular regions. The ISe line is blurred at the fovea (*asterisk*), but clearly observed in the peri-macular regions. The RPE is normal in the entire region. **c** An 83-year-old man. The COST line cannot be seen in the macula but is still visible in the peri-macular region. The ISe line is disrupted at the fovea (*asterisk*). There is an apparent thinning of the photoreceptor layer at the fovea. The RPE is normal in the entire region.

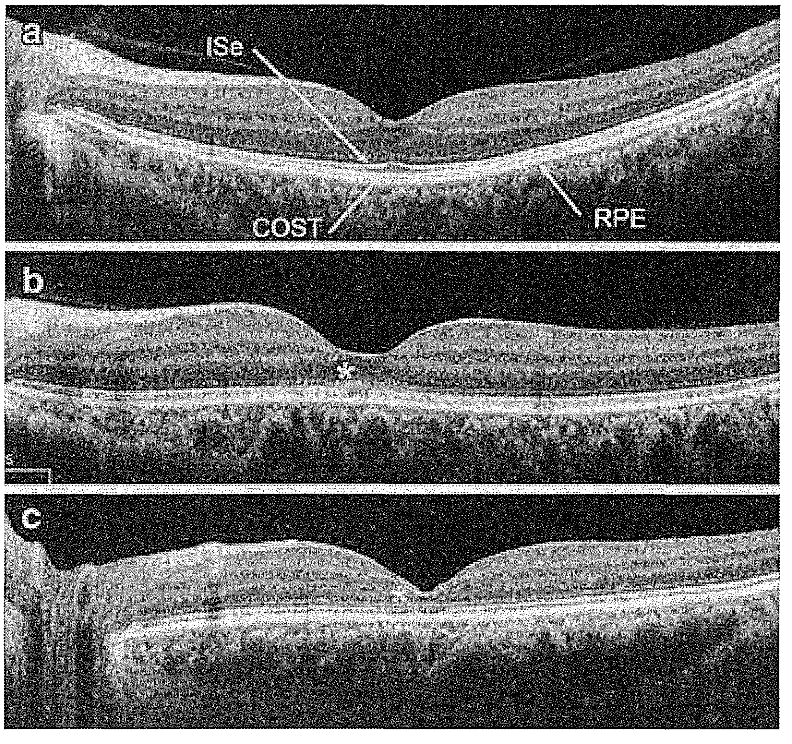

AQ2

The OCT images of sporadic cases of OMD without the *RP1L1* mutation, on the other hand, do not resemble those of patients with the *RP1L1* mutation. For example, some have a normal ISe line at the fovea, some a clearly localized disruption of the ISe line at the fovea, and some a minimally disrupted COST line at the fovea [30]. Considering that the OCT abnormalities in sporadic cases do not show similar patterns to patients with the *RP1L1* mutation, the phenotypically confirmed OMD eyes surely consist of diseases with multiple independent etiologies.

AQ3

Genetics

In 2010, linkage analyses in two OMD families with dominant inheritance patterns showed that mutations in the *RP1L1* gene located in the short arm of chromosome 8 were responsible for the OMD [31]. The cases with this mutation have been reported to share the same clinical features, especially the OCT images [30]. Recently, a number of cases of OMD with *RP1L* gene mutations have been reported [31, 39–42], and all of them had heterozygous missense mutations: the most common mutation was p.Arg45Trp in exon 2.

The *RP1L1* gene was originally cloned as a gene derived from common ancestors with the retinitis pigmentosa 1 (*RP1)* gene, which is responsible for 5–10 % of autosomal dominant retinitis pigmentosa (RP) worldwide. It is located on the same chromosome 8 [43–47]. An immunohistochemical study on cynomolgus monkeys showed that *RP1L1* was expressed in rod and cone photoreceptors, and it is believed to play important roles in the morphogenesis of the photoreceptors [43, 48]. Heterozygous *RP1L1* knock-out mice were reported to have normal retinal morphology while homozygous knock-out mice developed subtle retinal degeneration [48]. However, the RP1L1 protein has a very low degree of overall sequence identity (39 %) between humans and mice compared to the average values of sequence similarity observed between human and mice proteins. The cellular mechanisms that explain why only the macular region is impaired in human OMD patients have not been determined.

In the Japanese population, *RP1L1* gene mutations are rarely found in sporadic cases. There are OMD families without the *RP1L1* mutation where autosomal recessive inheritance is assumed. The genetic background leading to the OMD may be a variant, and other genetic causes will probably be determined in future studies.

Course of OMD

The correlation between age and visual acuity at the initial visit was not significant. In addition, the visual acuity of the older OMD patients in the same families was not always lower than those of the younger patients. These findings suggest that the age of onset and the speed of progression vary widely among patients even in the same family.

OMD is progressive in nature judging from the history of patients. However, only a few reports follow the eyes of OMD patients for a long period. The first patient diagnosed with OMD was a 29-year-old woman who was examined by one of the authors (YM) in 1986. Her fundus and fluorescein angiograms are still normal in 2014 although the visual acuity OU has decreased slightly.

Differential diagnosis

We believe that OMD may not be as rare as was originally thought. Before focal macular ERGs and mfERGs were used as routine clinical tests, many patients with OMD were probably misdiagnosed as having other diseases with low visual acuity and normal fundus. Because of the normal fundus appearances and normal full-field ERGs, OMD was often misdiagnosed as optic neuropathy of unknown origin, amblyopia, or non-organic visual loss. There were also cases with a diagnosis of senile cataract which were later diagnosed as OMD because the low visual acuity remained after the cataract surgery.

Cone dystrophy is a hereditary retinal dystrophy with progressive decrease of visual functions. Some of the patients with cone dystrophy may have normal fundus appearance [10]; however, eyes with cone dystrophy always have abnormal or absent full-field cone ERG as well as absent focal macular ERG. Congenital stationary night blindness with normal fundus is a hereditary retinal disease which is classified into two different clinical entities, complete and incomplete types [4]. This classification has been verified by molecular genetics analysis [5–9]. Most patients with both types often have moderate disturbances of visual acuity associated with high myopia or hyperopia from a young age. Some patients may not complain of night blindness, especially those with the incomplete type of CSNB [35]. Thus, a differential diagnosis of OMD is required. The full-field ERGs of both types show unique abnormalities [4, 49].

Future studies of OMD

In OMD patients, only the macular region is affected while other retinal regions remain normal functionally and morphologically, even at a very advanced stage. Moreover, the fundus appearance and retinal pigment epithelium remain intact until the end stage while the photoreceptor layer in the macular area is markedly damaged. Functionally, ON bipolar function is relatively preserved in macula of OMD patients with a depolarizing pattern in the focal macular ERGs. This finding may be related to a red–green color vision defect which was often observed in such OMD patients [15]. Also, the relative preservation of rod function in the macula may be from the result of some remodeling of the synapse from cone synapses to the ON synapses of rods.

These are still some important mysteries peculiar to OMD and not observed in other macular dystrophies. The *RP1L1* gene in humans has only 40 % homology with that of mice, and its cellular function in the primate's macula has not been determined. More detailed investigations on the function of *RP1L1* should provide information to answer these questions.

Acknowledgments

This research was supported by (1) research grants from the Ministry of Health, Labor and Welfare, Japan and (2) Grant-in-Aid for Scientific Research, Japan Society for the Promotion of Science, Japan. This manuscript was edited by Prof. Duco Hamasaki of the Bascom Palmer Institute.

Conflicts of interest

Y. Miyake, None; K. Tsunoda, None.

References

1.

Oguchi C. Ueber eine Abart von Hemeralopie. Acta Soc Ophthalmol Jpn. 1907;11:123–34 (in Japanese).

2.

Takayasu M. A case with peculiar changes of the central retinal vessels. Acta Soc Ophthalmol Jpn. 1908;12:554 (in Japanese).

3.

Harada E. Beitrag zur klinischen von nichteitriger Choroiditis (choroiditis diffusa acuta). Acta Soc Ophthalmol Jpn. 1926;30:356–78 (in Japanese).

4.

Miyake Y, Yagasaki K, Horiguchi M, Kawase Y, Kanda T. Congenital stationary night blindness with negative electroretinogram. A new classification. Arch Ophthalmol. 1986;104:1013–20.

5.

Bech-Hansen NT, Naylor MJ, Maybaum TA, Pearce WG, Koop B, Fishman GA, et al. Loss-of-function mutations in a calcium-channel alpha1-subunit gene in Xp11.23 cause incomplete X-linked congenital stationary night blindness. Nat Genet. 1998;19:264–7.

6.

Bech-Hansen NT, Naylor MJ, Maybaum TA, Sparkes RL, Koop B, Birch DG, et al. Mutations in NYX, encoding the leucine-rich proteoglycan nyctalopin, cause X-linked complete congenital stationary night blindness. Nat Genet. 2000;26:319–23.

7.

Boycott KM, Pearce WG, Musarella MA, Weleber RG, Maybaum TA, Birch DG, et al. Evidence for genetic heterogeneity in X-linked congenital stationary night blindness. Am J Hum Genet. 1998;62:865–75.

8.
Pusch CM, Zeitz C, Brandau O, Pesch K, Achatz H, Feil S, et al. The complete form of X-linked congenital stationary night blindness is caused by mutations in a gene encoding a leucine-rich repeat protein. Nat Genet. 2000;26:324–7.
9.
Strom TM, Nyakatura G, Apfelstedt-Sylla E, Hellebrand H, Lorenz B, Weber BH, et al. An L-type calcium-channel gene mutated in incomplete X-linked congenital stationary night blindness. Nat Genet. 1998;19:260–3.
10.
Miyake Y. Cone dystrophy. In: Electrodiagnosis of retinal diseases. Tokyo: Springer-Verlag; 2006.
11.
Miyake Y. Rod monochromacy. In: Electrodiagnosis of retinal diseases. Tokyo: Springer-Verlag; 2006.
12.
Terasaki H, Miyake Y. Japanese family with blue cone monochromatism. Jpn J Ophthalmol. 1992;36:132–41.
13.
Miyake Y, Ichikawa K, Shiose Y, Kawase Y. Hereditary macular dystrophy without visible fundus abnormality. Am J Ophthalmol. 1989;108:292–9.
14.
Miyake Y, Horiguchi M, Tomita N, Kondo M, Tanikawa A, Takahashi H, et al. Occult macular dystrophy. Am J Ophthalmol. 1996;122:644–53.
15.
Miyake Y. Occult macular dystrophy. In: Electrodiagnosis of retinal diseases. Tokyo: Springer-Verlag; 2006.
16.
Miyake Y. Studies of local macular ERG. Nihon Ganka Gakkai Zasshi. 1988;92:1419–49.
17.
Miyake Y, Awaya S. Stimulus deprivation amblyopia. Simultaneous recording of local macular electroretinogram and visual evoked response. Arch Ophthalmol. 1984;102:998–1003.
18.
Miyake Y, Shiroyama N, Horiguchi M, Ota I. Asymmetry of focal ERG in

human macular region. Invest Ophthalmol Vis Sci. 1989;30:1743–9.
19.
Miyake Y, Shiroyama N, Ota I, Horiguchi M. Oscillatory potentials in electroretinograms of the human macular region. Invest Ophthalmol Vis Sci. 1988;29:1631–5.
20.
Miyake Y, Yanagida K, Kondo M, Ota I. Subjective scotometry and recording local macular electroretinogram and visual evoked response. Jpn J Ophthalmol. 1981;25:438–48.
21.
Sutter EE, Tran D. The field topography of ERG components in man I. The photopic luminance response. Vision Res. 1992;32:433–46.
22.
Fujii S, Escano MF, Ishibashi K, Matsuo H, Yamamoto M. Multifocal electroretinography in patients with occult macular dystrophy. Br J Ophthalmol. 1999;83:879–80.
23.
Piao CH, Kondo M, Tanikawa A, Terasaki H, Miyake Y. Multifocal electroretinogram in occult macular dystrophy. Invest Ophthalmol Vis Sci. 2000;41:513–7.
24.
Wildberger H, Niemeyer G, Junghardt A. Multifocal electroretinogram (mfERG) in a family with occult macular dystrophy (OMD). Klin Monatsbl Augenheilkd. 2003;220:111–5.
25.
Kondo M, Ito Y, Ueno S, Piao CH, Terasaki H, Miyake Y. Foveal thickness in occult macular dystrophy. Am J Ophthalmol. 2003;135:725–8.
26.
Brockhurst RJ, Sandberg MA. Optical coherence tomography findings in occult macular dystrophy. Am J Ophthalmol. 2007;143:516–8.
27.
Koizumi H, Maguire JI, Spaide RF. Spectral domain optical coherence tomographic findings of occult macular dystrophy. Ophthalmic Surg Lasers Imaging. 2009;40:174–6.
28.
Lubinski W, Goslawski W, Penkala K, Drobek-Slowik M, Karczewicz D. A

43-year-old man with reduced visual acuity and normal fundus: occult macular dystrophy–case report. Doc Ophthalmol. 2008;116:111–8.
29.
Park SJ, Woo SJ, Park KH, Hwang JM, Chung H. Morphologic photoreceptor abnormality in occult macular dystrophy on spectral-domain optical coherence tomography. Invest Ophthalmol Vis Sci. 2010;51:3673–9.
30.
Tsunoda K, Usui T, Hatase T, Yamai S, Fujinami K, Hanazono G, et al. Clinical characteristics of occult macular dystrophy in family with mutation of Rp1l1 gene. Retina-J Retinal Vitreous Dis. 2012;32:1135–47.
31.
Akahori M, Tsunoda K, Miyake Y, Fukuda Y, Ishiura H, Tsuji S, et al. Dominant mutations in RP1L1 are responsible for occult macular dystrophy. Am J Hum Genet. 2010;87:424–9.
32.
Viswanathan S, Frishman LJ, Robson JG, Harwerth RS, Smith EL 3rd. The photopic negative response of the macaque electroretinogram: reduction by experimental glaucoma. Invest Ophthalmol Vis Sci. 1999;40:1124–36.
33.
Fujinami K, Tsunoda K, Hanazono G, Shinoda K, Ohde H, Miyake Y. Fundus autofluorescence in autosomal dominant occult macular dystrophy. Arch Ophthalmol. 2011;129:597–602.
34.
Sieving PA. Photopic ON- and OFF-pathway abnormalities in retinal dystrophies. Trans Am Ophthalmol Soc. 1993;91:701–73.
35.
Jacobson SG, Voigt WJ, Parel JM, Apathy PP, Nghiem-Phu L, Myers SW, et al. Automated light- and dark-adapted perimetry for evaluating retinitis pigmentosa. Ophthalmology. 1986;93:1604–11.
36.
Srinivasan VJ, Adler DC, Chen YL, Gorczynska I, Huber R, Duker JS, et al. Ultrahigh-speed optical coherence tomography for three-dimensional and en face imaging of the retina and optic nerve head. Invest Ophthalmol Vis Sci. 2008;49:5103–10.
37.

Anderson DH, Fisher SK, Steinberg RH. Mammalian cones—disk shedding, phagocytosis, and renewal. Invest Ophthalmol Vis Sci. 1978;17:117–33.
38.
Fernandez EJ, Hermann B, Povazay B, Unterhuber A, Sattmann H, Hofer B, et al. Ultrahigh resolution optical coherence tomography and pancorrection for cellular imaging of the living human retina. Opt Express. 2008;16:11083–94.
39.
Kabuto T, Takahashi H, Goto-Fukuura Y, Igarashi T, Akahori M, Kameya S, et al. A new mutation in the RP1L1 gene in a patient with occult macular dystrophy associated with a depolarizing pattern of focal macular electroretinograms. Mol Vis. 2012;18:1031–9.
40.
Hayashi T, Gekka T, Kozaki K, Ohkuma Y, Tanaka I, Yamada H, et al. Autosomal dominant occult macular dystrophy with an RP1L1 mutation (R45W). Optom Vis Sci: Off Publ Am Acad Optom. 2012;89:684–91.
41.
Ahn SJ, Cho SI, Ahn J, Park SS, Park KH, Woo SJ. Clinical and genetic characteristics of Korean occult macular dystrophy patients. Invest Ophthalmol Vis Sci. 2013;54:4856–63.
42.
Davidson AE, Sergouniotis PI, Mackay DS, Wright GA, Waseem NH, Michaelides M, et al. RP1L1 variants are associated with a spectrum of inherited retinal diseases including retinitis pigmentosa and occult macular dystrophy. Hum Mutat. 2013;34:506–14.
43.
Conte I, Lestingi M, den Hollander A, Alfano G, Ziviello C, Pugliese M, et al. Identification and characterisation of the retinitis pigmentosa 1-like1 gene (RP1L1): a novel candidate for retinal degenerations. Eur J Human Genet : EJHG. 2003;11:155–62.
44.
Bowne SJ, Daiger SP, Malone KA, Heckenlively JR, Kennan A, Humphries P, et al. Characterization of RP1L1, a highly polymorphic paralog of the retinitis pigmentosa 1 (RP1) gene. Mol Vis. 2003;9:129–37.
45.

Pierce EA, Quinn T, Meehan T, McGee TL, Berson EL, Dryja TP. Mutations in a gene encoding a new oxygen-regulated photoreceptor protein cause dominant retinitis pigmentosa. Nat Genet. 1999;22:248–54.
46.
Sullivan LS, Heckenlively JR, Bowne SJ, Zuo J, Hide WA, Gal A, et al. Mutations in a novel retina-specific gene cause autosomal dominant retinitis pigmentosa. Nat Genet. 1999;22:255–9.
47.
Jacobson SG, Cideciyan AV, Iannaccone A, Weleber RG, Fishman GA, Maguire AM, et al. Disease expression of RP1 mutations causing autosomal dominant retinitis pigmentosa. Invest Ophthalmol Vis Sci. 2000;41:1898–908.
48.
Yamashita T, Liu J, Gao J, LeNoue S, Wang C, Kaminoh J, et al. Essential and synergistic roles of RP1 and RP1L1 in rod photoreceptor axoneme and retinitis pigmentosa. J Neurosci. 2009;29:9748–60.
49.
Miyake Y. Establishment of the concept of new clinical entities—complete and incomplete form of congenital stationary night blindness. Nihon Ganka Gakkai Zasshi. 2002;106:737–55 (discussion 56).

PROOF COVER SHEET

Author(s): Satoshi Katagiri, Takaaki Hayashi, Kazutoshi Yoshitake, Yuri Sergeev, Masakazu Akahori, Masaaki Furuno, Jo Nishino, Kazuho Ikeo, Kazushige Tsunoda, Hiroshi Tsuneoka, and Takeshi Iwata

Article title: Congenital Achromatopsia and Macular Atrophy Caused by a Novel Recessive *PDE6C* Mutation (p.E591K)

Article no: NOPG_A_991932

Enclosures: 1) Query sheet
2) Article proofs

Dear Author,
Please check these proofs carefully. It is the responsibility of the corresponding author to check against the original manuscript and approve or amend these proofs. A second proof is not normally provided. Informa Healthcare cannot be held responsible for uncorrected errors, even if introduced during the composition process. The journal reserves the right to charge for excessive author alterations, or for changes requested after the proofing stage has concluded.

The following queries have arisen during the editing of your manuscript and are marked in the margins of the proofs. Unless advised otherwise, submit all corrections using the CATS online correction form. Once you have added all your corrections, please ensure you press the "Submit All Corrections" button.

Please review the table of contributors below and confirm that the first and last names are structured correctly and that the authors are listed in the correct order of contribution.

Contrib. No.	Prefix	Given name(s)	Surname	Suffix
1		Satoshi	Katagiri	
2		Takaaki	Hayashi	
3		Kazutoshi	Yoshitake	
4		Yuri	Sergeev	
5		Masakazu	Akahori	
6		Masaaki	Furuno	
7		Jo	Nishino	
8		Kazuho	Ikeo	
9		Kazushige	Tsunoda	
10		Hiroshi	Tsuneoka	
11		Takeshi	Iwata	

AUTHOR QUERIES

Q1: Give the volume number and page span for Ref. 1?

Q2: Please provide volume number.

Q3: Please provide last page range.

Ophthalmic Genetics, Early Online, 1–8, 2015
© Informa Healthcare USA, Inc.
ISSN: 1381-6810 print / 1744-5094 online
DOI: 10.3109/13816810.2014.991932

informa healthcare

RESEARCH REPORT

Congenital Achromatopsia and Macular Atrophy Caused by a Novel Recessive *PDE6C* Mutation (p.E591K)

Satoshi Katagiri[1,2], Takaaki Hayashi[2], Kazutoshi Yoshitake[3], Yuri Sergeev[4], Masakazu Akahori[1], Masaaki Furuno[5], Jo Nishino[3], Kazuho Ikeo[3], Kazushige Tsunoda[6], Hiroshi Tsuneoka[2], and Takeshi Iwata[1]

[1]*Division of Molecular and Cellular Biology, National Institute of Sensory Organs, National Hospital Organization Tokyo Medical Center, Tokyo, Japan,* [2]*Department of Ophthalmology, The Jikei University School of Medicine, Tokyo, Japan,* [3]*Laboratory of DNA Data Analysis, National Institute of Genetics, Shizuoka, Japan,* [4]*National Eye Institute, National Institutes of Health, Bethesda, MD, USA,* [5]*RIKEN Center for Life Science Technologies, Division of Genomic Technologies, Life Science Accelerator Technology Group, Transcriptome Technology Team, Yokohama, Japan, and* [6]*Laboratory of Visual Physiology, National Institute of Sensory Organs, National Hospital Organization Tokyo Medical Center, Tokyo, Japan*

ABSTRACT

Purpose: We have previously reported clinical features of two siblings, a sister with complete achromatopsia (ACHM) and a brother with incomplete ACHM, in a consanguineous Japanese family. With the current study, we intended to identify a disease-causing mutation in the siblings and to investigate why the phenotypes of the siblings differed.

Methods: We performed a comprehensive ophthalmic examination for each sibling and parent. Whole-exome and Sanger sequencing were performed on genomic DNA. Molecular modeling was analyzed in an *in silico* study.

Results: The ophthalmic examination revealed severe macular atrophy in the older female sibling at 30 years of age and mild macular atrophy in the brother at 26 years of age. The genetic analysis identified a novel homozygous *PDE6C* mutation (p.E591K) as the disease-causing allele in the siblings. Each parent was heterozygous for the mutation. Molecular modeling showed that the mutation could cause a conformational change in the PDE6C protein and result in reduced phosphodiesterase activity. We also identified an *OPN1SW* mutation (p.G79R), which is associated with congenital tritan deficiencies, in the sister and the father but not in the brother.

Conclusions: A novel homozygous *PDE6C* mutation was identified as the cause of ACHM. In addition, we identified an *OPN1SW* mutation in the sibling with complete ACHM, which might explain the difference in phenotype (complete versus incomplete ACHM) between the siblings.

Keywords: Achromatopsia, *OPN1SW*, *PDE6C*, *RHO*, whole-exome sequencing

INTRODUCTION

Congenital achromatopsia (ACHM) (ACHM2: OMIM #216900, ACHM3: OMIM #262300, ACHM4: OMIM #613856, ACHM5/COD4: OMIM #613093, and ACHM6/RCD3A: OMIM #610024) is an autosomal recessive disorder with an estimated frequency of 1:30,000 to 1:50,000.[1] ACHM is characterized by low visual acuity, nystagmus, photophobia, severe color vision defects, and reduced or absent cone responses

Received 28 September 2014; revised 24 October 2014; accepted 15 November 2014; published online ▌▌▌

Correspondence: Takaaki Hayashi, MD, PhD, Department of Ophthalmology, The Jikei University School of Medicine, 3-25-8 Nishi-shimbashi, Minato-ku, Tokyo 105-8461, Japan. Tel: +81 3 3433 1111 (ext. 3581). Fax: +81 3 5378 8828. E-mail: taka@jikei.ac.jp

despite normal rod responses on electroretinography.[2–5] Fundus appearance is usually normal, although macular pigmentary changes and atrophy have been described.[6]

Mutations in five genes have been identified as causes of ACHM: cyclic nucleotide-gated channel alpha-3 (*CNGA3)*, cyclic nucleotide-gated channel beta-3 *(CNGB3)*, guanine nucleotide-binding protein, alpha-transducing activity polypeptide 2 *(GNAT2)*, phosphodiesterase 6C (*PDE6C)*, and phosphodiesterase 6H (*PDE6H*).[7–13] A previous study found that *CNGB3* mutations account for half of the studied ACHM cases (48.2%), *CNGA3* mutations account for 28.7%, *GNAT2* mutations account for 2.2%, and *PDE6C* mutations account for only 1.4%.[14] However, another studies report that mutations in *CNGB3* account for 87% of ACHM cases, *CNGA3* for 5%, and *PDE6C* for less than 1%; and they found no mutations in *GNAT2*.[12,13,15] The proteins encoded by these five genes are exclusively expressed in cone photoreceptors, where they are involved in the cone phototransduction cascade.

We have previously described two Japanese ACHM siblings with different clinical phenotypes.[16] In the present study, using whole-exome sequence analysis, we investigated disease-causing mutation and genetic background to clarify the different clinical phenotypes between the siblings. Additionally, *in silico* molecular modeling was conducted to investigate the impact of the disease-causing mutation.

METHODS

The protocol used for this study was approved by the Institutional Review Board of the Jikei University School of Medicine and National Hospital Organization Tokyo Medical Center. The protocol adhered to the tenets of the Declaration of Helsinki, and informed consent was obtained from each participant.

Clinical Studies

We studied the affected two siblings, each with ACHM, in one consanguineous Japanese pedigree (JU#0149-110JIKEI). Their non-ACHM father (III-1) and mother (III-2) were first cousins. We performed a complete ophthalmic examination, including decimal best-corrected visual acuity (BCVA), funduscopy, Goldmann visual-field and color-vision testing, fundus autofluorescence imaging (FAI) (Spectralis HRA; Heidelberg Engineering, Heidelberg, Germany), optical coherence tomography (OCT) (Carl Zeiss Meditec AG, Dublin, CA), and full-field and spectral electroretinography (ERG). Under light-adapted conditions, spectral (L/M- and S-cone) ERG was recorded using a light-emitting diode built-in contact lens electrode (LS-C, Mayo, Aichi, Japan) as previously described.[17] Briefly, responses were evoked by blue (430 nm) stimuli (63.0 cd/m^2) or red (644 nm) stimuli (63.0 cd/m^2) under a white (2.0 log cd/m^2) background. Stimulus duration (3 milliseconds) and frequency (4.850 Hz) were specified; the band pass was 1 to 300 Hz; the PuREC system (Mayo) was used to average 300 signals.[16]

Molecular Genetic Studies

We extracted genomic DNA from each affected sibling and each parent. Whole-exome sequencing was performed on the four family members. The obtained data were filtered to identify disease-causing mutations as previously described in detail.[18–20] In addition, we assessed any variants that were found in 220 genes registered in the RetNet database (https://sph.uth.edu/retnet/). We identified putative disease-causing mutations in three genes, *PDE6C, OPN1SW,* and *RHO*; each mutation was confirmed via Sanger sequencing. The *PDE6C, OPN1SW,* and *RHO* sequence was compared with the NCBI Reference Sequence for each transcript (GenBank NM_006204.3, NM_001708.2, and NM_000539.3 respectively).

Molecular Modeling

The amino acid sequence of PDE6C was retrieved from the UniProtKB database (http://www.uniprot.org/uniprot/P51160). The PDE6C domain structure was generated with the automated protein-homology modeling server Swiss-Model (http://swissmodel.expasy.org) by using dimeric cGMP-dependent 3′,5′-cyclic phosphodiesterase (PDE2A) as a structural template (Protein Data Bank file: 3ibj). Mutant variant structure, p.E591K, was generated as a dimer, refined, 10-ns equilibrated at 37 °C using a 149.4 Å × 118.2 Å × 89.8 Å water box, and Yasara 2 force field implicated in a molecular visualization, modeling, and dynamics program called YASARA.[21] Molecular visualization was also performed by using the UCSF Chimera.[22]

RESULTS

Ophthalmological Findings

The older sister (patient IV-1) and the younger brother (patient IV-2) were diagnosed with complete and incomplete ACHM, respectively. Detailed clinical features of the siblings from 7 to 21 and from 5 to 18 years of age (IV-1 and VI-2, respectively) have been described previously.[16]

COLOR Online / B&W in Print

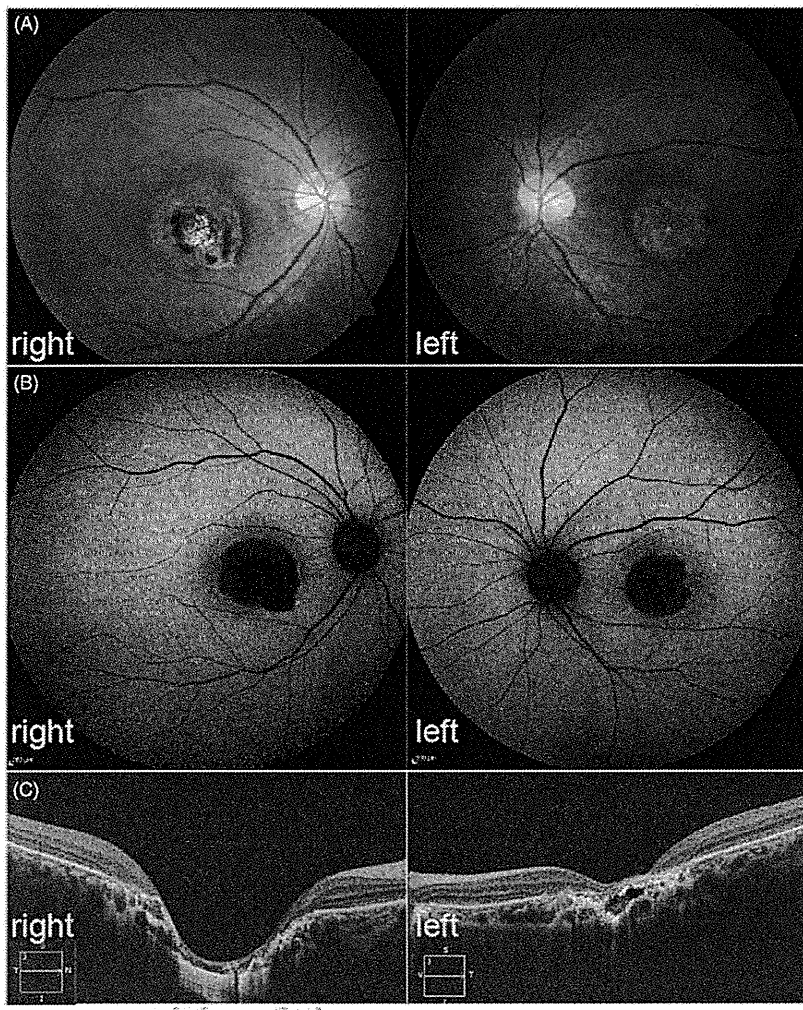

FIGURE 1. Fundus images of patient IV-1 who has complete achromatopsia at 30 years of age. Fundus photographs (A), fundus autofluorescence images (B), and optical coherence tomography (C).

Patient IV-1[16] is currently 30 years of age. Her BCVA was 0.2 (with moderate myopia) in her right and 0.1 (with moderate myopia) in her left eyes. Funduscopy showed atrophic chorioretinal macular scarring in the right eye and macular atrophy in the left eye (Figure 1A). FAI revealed complete loss of autofluorescence in the macular lesions of both eyes (Figure 1B). OCT revealed severe macular thinning of all layers in both eyes and retinal and choroidal excavation in the right eye (Figure 1C). At the age of 31, visual field testing showed bilateral central scotomas (5–10 degrees) of the I-3e or I-2e isopters, but the peripheral visual fields of the I-5e and I-4e isopters were normal (data not shown). The central scotomas at 31 years of age had broadened slightly relative to that at 11 years of age.

Patient IV-2 was diagnosed with incomplete ACHM at the age of 5.[16] At present, the patient is 26 years old. His BCVA was 0.2 (with high hyperopia) in each eye. Funduscopy showed atrophic macular changes in both eyes (Figure 2A). Fundus autofluorescence imaging revealed hyper-autofluorescent areas of the maculas in both eyes (Figure 2B). Optical coherence tomography revealed retinal thinning with loss of the outer retinal layer in each macula (Figure 2C). Visual field testing showed bilateral central (5 degrees) scotomas of the I-3e or I-2e isopters, but the peripheral visual fields of the I-5e and I-4e isopters were normal (data not shown), demonstrating that there was little change in the visual field between 26 and 12 years of age.

The father (III-1) reported no visual disturbance until the age of 63 years; he has since undergone comprehensive ophthalmic examinations. His BCVA was 1.2 (with moderate hyperopia) in each eye. In the anterior segments and media, there were mild senior cataracts in both eyes. Funduscopy and OCT showed normal appearance except for some macular drusen in

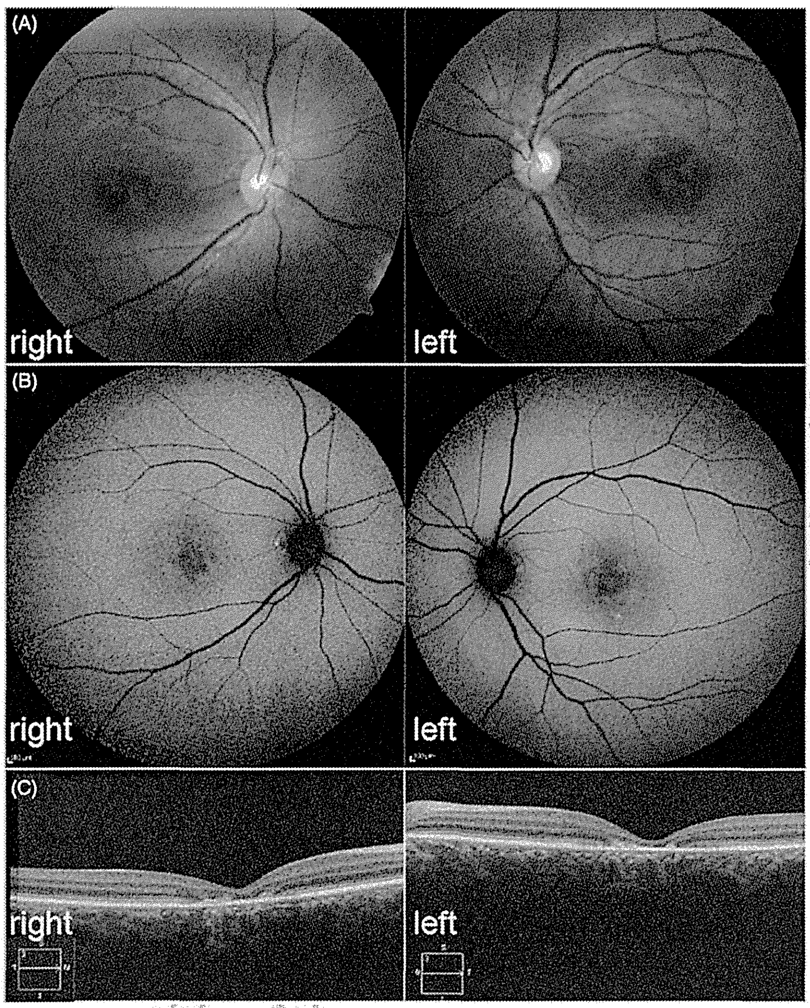

FIGURE 2. Fundus images of patient IV-2 who has incomplete achromatopsia at 26 years of age. Fundus photographs (A), fundus autofluorescence imaging (B), and optical coherence tomography (C).

both eyes. Color vision tests were performed monocularly for each eye. He identified all plates on the Ishihara test. Panel D-15 showed that he had minor errors in the right eye, and no errors in the left eye. In the F-M 100-hue tests, the square roots calculated from the total error scores were 15.2 (right eye) and 11.5 (left eye). The average in a group of 60- to 69-year-olds with normal color vision and good visual acuity is reportedly 10.0–11.0.[23–25] His orientation axes were 5.16 (right eye) and 4.84 (left eye), indicating blue-yellow (or tritan) color vision deficiencies.[25] Although the full-field ERG showed normal rod and cone responses in both eyes, S-cone responses by blue stimulus were not evident in the left (Figure 3) and right eyes, whereas L/M-cone responses by red stimulus were evident in the left (Figure 3) and right eyes.

The mother (III-2) reported no visual disturbance until the age of 54 years. Her BCVA was 1.2 (with moderate hyperopia) in each eye. Anterior segments, funduscopy, and OCT showed normal appearance in both eyes.

Identification of Gene Mutations

After the filtering steps, only one *PDE6C* mutation remained. Subsequently, in each sibling, we identified a novel homozygous mutation (c.1771G>A, p.E591K) in exon 14 of the *PDE6C* gene. Each parent was heterozygous for the mutant allele. This novel mutation (p.E591K) was not found in the Single Nucleotide Polymorphism Database, the 1000 Genomes database, the Human Genetic Variation Browser, or the Human Gene Mutation Database. No pathological mutations were detected in the *CNGA3*, *CNGB3*, *GNAT2*, or *PDE6H* genes, which are each known as causative genes for ACHM.

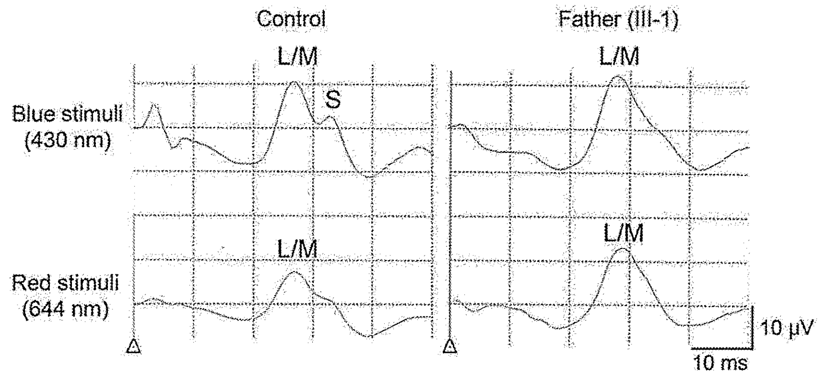

FIGURE 3. Spectral electroretinography in a control and the father (III-1). In the left eye of the father (III-1), S-cone responses by blue stimulus (−0.72 log cd·second/m^2) are not detectable, whereas L/M-cone responses by red stimulus (−0.72 log cd·second/m^2) are preserved.

Specifically we focused on the 220 genes registered in the RetNet database and found that this family harbored 11 registered mutations or variants (Supplementary Table S1 – online only). Interestingly, there were two known disease-causing mutations (p.G79R in *OPN1SW* and p.T193M in *RHO*),[26,27] and each was heterozygous in this instance. The p.G79R mutation in *OPN1SW* reportedly causes congenital tritan color vision deficiencies,[27] while p.T193M in *RHO* reportedly causes autosomal dominant retinitis pigmentosa.[26] The father (III-1) and patient IV-1 each had both mutations; the mother (III-2) and patient IV-2 had neither mutation. Each genomic mutation in *PDE6C, OPN1SW,* and *RHO* was confirmed by Sanger sequencing (Supplementary Figure S1 – online only).

Protein Structure and Function Analysis

The PDE6C sequence showed 22.5% sequence identity to PDE2A, which was used as a structural template to model residues 57-816 of PDE6C. PDE6C, like PDE2A, includes GAF-A, GAF-B, and the PDEase catalytic domain (Figure 4A). The catalytic domain has a binding site for divalent Zn^{2+} cations. Results of simulated annealing of the mutant variant p.E591K are shown in Figure 4B. The p.E591K mutation replaced a negatively-charged glutamic acid with a positively-charged lysine residue. This alteration dramatically changes the interaction between two helices, H5 and H12, located within the catalytic domain (Figure 4C). Indeed, in wild-type protein, negatively charged glutamic acid E591 (OE1 atom) forms a salt bridge (∼3 Å distance) with positively charged lysine K711 (NZ atom). The p.E591K mutation introduced a positive charge at position 591 and was predicted to break the salt bridge. This resulted in a conformational change caused by the repulsive force between K711 and K591 side chains, which increases the interatomic distance between two chains up to 6.9 Å in the mutant variant. The breaking of the salt bridge would destabilize the hydrophobic interaction between H5 and H12 helices and cause a change in Zn^{2+} cation coordination (Figure 4B).

DISCUSSION

Here, using whole-exome sequence analysis, we identified a novel *PDE6C* mutation (p.E591K) in two siblings with ACHM and macular atrophy.

PDE6C has two GAF domains (GAF-A and GAF-B) and one PDEase catalytic domain. The p.E591K mutation was located in the PDEase catalytic domain. The E591 residue is highly conserved among vertebrates (Supplementary Figure S1). Therefore, it is possible that the amino acid change from a negatively-charged glutamic acid to a positively-charged lysine may cause loss of PDE6C function. As shown in the functional analysis of molecular modeling, the p.E591K mutation could potentially decrease metal cation binding and might affect the catalytic function of PDE6C. The results of this modeling analysis were consistent with results of a structural study of phosphodiesterase inhibition by the C-terminal region of the γ-subunit.[28] In our PDE6C model, the H5 and H12 helices were positioned close to the H- and M-loops, residues 610-632 and 748-770, respectively. These loops formed a distinct interface that contributed to the γ-subunit binding site. The disruption of this interface causes retinal degeneration in *atrd3* mice.[29,30] Our findings indicated that the H5 and H12 helices might be involved in the stabilization of the γ-subunit binding site. PDE6C plays an important role in cone photoreceptors by rapidly decreasing intracellular levels of the second messenger cGMP. Reportedly, known *PDE6C* gene mutations reduce PDE activity, based on data from a PDE5/PDE6 chimeric protein expressed in Sf9 insect cells.[14,31,32] Therefore, the